Oscillations in the inflaton potential: Exact numerical analysis and comparison with the recent and forthcoming CMB datasets

Moumita Aich[1]*, Dhiraj Kumar Hazra[2]†, L. Sriramkumar[2]‡ and Tarun Souradeep[1]§
[1] *IUCAA, Post Bag 4, Ganeshkhind, Pune 411007, India.*
[2] *Harish-Chandra Research Institute, Chhatnag Road, Jhunsi, Allahabad 211019, India.*
(Dated: June 15, 2011)

Amongst the multitude of inflationary models currently available, models that lead to features in the primordial scalar spectrum are drawing increasing attention, since certain features have been found to provide a better fit to the CMB data than the conventional, nearly scale invariant, primordial spectrum. In this work, we carry out an exact numerical analysis of two models that lead to oscillations *over all scales* in the scalar power spectrum. We consider the model described by a quadratic potential which is superposed by a sinusoidal modulation and the recently popular axion monodromy model. Since the oscillations continue even onto smaller scales, in addition to the WMAP data, we also compare the models with the small scale data from ACT. Though, both the models, broadly, result in oscillations in the spectrum, interestingly, we find that, while the monodromy model leads to a considerably better fit to the data in comparison to the standard power law spectrum, the quadratic potential superposed with a sinusoidal modulation does not improve the fit to a similar extent. We also carry out forecasting of the parameters using simulated Planck data for both the models. We show that the Planck mock data performs better in constraining the model parameters as compared to the presently available CMB datasets.

PACS numbers: 98.80.Cq, 98.70.Vc, 04.30.-w

I. LOCAL VERSUS NON-LOCAL FEATURES IN THE PRIMORDIAL SPECTRUM

Inflation has proven to be the most efficient mechanism to overcome difficulties such as the horizon and the flatness problems that plague the standard, hot, big bang cosmological model. Importantly, in addition to resolving such issues, inflation successfully generates primordial fluctuations which seed the formation of structures. Over the years, numerous models have been proposed that lead to a sufficient duration of inflation and also produce perturbations of suitable amplitude and shape that are consistent with the observations of the anisotropies in the Cosmic Microwave Background (CMB) [1–3] as well as other observational bounds. Currently, many of the models that lead to slow roll inflation and, therefore, to a nearly scale invariant primordial spectrum, seem to perform equally well against the available data [4]. The hope remains that further CMB data from the present and forthcoming missions such as Planck [5] and the Cosmic Origins Explorer [6] may help us discriminate better between the various models.

Although, a nearly scale invariant power spectrum predicted by slow roll inflation, along with the background ΛCDM model, matches the angular spectrum from the CMB observations quite well, there exists a few outliers (notably, near the multipole moments of $\ell = 2$, 22 and 40) in the Wilkinson Microwave Anisotropy Probe (WMAP) data [1, 2]. Interestingly, model independent reconstruction of the primordial spectrum from the observed pattern of the CMB anisotropies seem to suggest the possible presence of specific features in the spectrum (see Refs. [7]; for a different view, see Refs. [8]). Moreover, it has been found that certain localized features actually lead to a better fit to the data than the conventional power law spectrum (in this context, see, for instance, Refs. [9–13]). And, it should be noted here that generating such features require either one or more periods of deviation from slow roll inflation [14–16] or modifications to the initial conditions on the perturbations [17].

Apart from localized features, it is interesting to examine whether the CMB data also point to non-local features—i.e. certain characteristic and repeated behavior that extend over a wide range of scales—in the primordial spectrum. A quick glance at the unbinned CMB data seems to suggest that, after all, such an eventuality need not altogether be surprising. In fact, earlier investigations on possible Planck scale modifications to the primordial spectrum have indicated that continuing oscillations in the power spectrum can lead to a substantial improvement in the fit at the cost of two or three additional parameters [18]. In this work, we shall investigate two inflationary models that lead to similar oscillations over all scales in the curvature perturbation spectrum. We shall consider a model described by the conventional quadratic potential, but superposed by a sinusoidal modulation [19], and the presently popular axion monodromy model (see, for example, Refs. [20]). It should be mentioned here that these models have been compared with the WMAP data recently [19–21]. However, all the ear-

*E-mail: moumita@iucaa.ernet.in
†E-mail: dhiraj@hri.res.in
‡Current address: Department of Physics, Indian Institute of Technology Madras, Chennai 600036, India. E-mail: sriram@physics.iitm.ac.in
§E-mail: tarun@iucaa.ernet.in

lier analyses had resorted to evaluating the scalar power spectrum in the slow roll approximation. In contrast, we shall compute the scalar power spectrum *exactly* using a highly accurate numerical code. And, we shall evaluate the tensor spectrum too accurately and include it in our analysis. Moreover, as the oscillations in the inflationary scalar power spectrum continue even over smaller scales, in addition to the WMAP seven year data [2], we shall compare the models with the small scale data from the Atacama Cosmology Telescope (ACT) [3]. We shall also arrive at the constraints on the model parameters using simulated Planck data. While both the models that we consider lead to oscillations in the spectrum, we find that the monodromy model results in a superior fit to the data. Further, as we shall see, the Planck mock data leads to better constraints on the model parameters than the currently available CMB datasets.

This paper is organized as follows. In the following section, we shall briefly describe the models that we shall consider and the methodology that we shall adopt to compare the models with the data. In the subsequent two sections, we shall present the results of our analysis and examine whether Planck will be able to constrain the models better, respectively. We shall conclude with a brief summary and discussion in the final section.

Note that we shall work in units such that $\hbar = c = (8\,\pi\,G) = 1$. Moreover, we shall assume the background cosmological model to be the standard, spatially flat, ΛCDM model.

II. MODELS AND METHODOLOGY

In this section, we shall briefly describe the models that we shall work with and the methodology we shall adopt to compare the models with the data.

A. The models

As we mentioned, we shall consider two models, the first of which is the chaotic inflationary that is modulated by sinusoidal oscillations [19]. The model is described by the potential

$$V(\phi) = \frac{1}{2}\,m^2\,\phi^2\left[1 + \alpha\,\sin\left(\frac{\phi}{\beta} + \delta\right)\right], \tag{1}$$

where, evidently, m is the parameter that characterizes the original quadratic potential, while the parameters α and β describe the amplitude and the frequency of the superimposed oscillations. We have also included the parameter δ, which shifts the oscillations within one period, in our analysis. The second model that we shall consider is the axion monodromy model which is motivated by string theory [20–22]. The inflaton potential in such a case is given by

$$V(\phi) = \lambda\,\left[\phi + \alpha\,\cos\left(\frac{\phi}{\beta} + \delta\right)\right]. \tag{2}$$

Note that, while the amplitude of the oscillation is fixed in the axion monodromy model, in the chaotic model described by the potential (1), the amplitude depends quadratically on the field. The inflaton oscillates as it rolls down these potentials, and these oscillations continue all the way until the end of inflation. This behavior leads to small oscillations in the slow roll parameters, which in turn results in continuing oscillations in the primordial scalar power spectrum. Our goal is to examine the extent to which such oscillations are admitted by the CMB data.

We shall compare the performance of the above two inflationary models with the conventional, power law, primordial spectrum. Recall that, the power law, scalar and tensor spectra are usually written as (see, for example, Refs. [23, 24])

$$\mathcal{P}_{_{\rm S}}(k) = A_{_{\rm S}}\left(\frac{k}{k_0}\right)^{n_{_{\rm S}}-1} \quad \text{and} \quad \mathcal{P}_{_{\rm T}}(k) = A_{_{\rm T}}\left(\frac{k}{k_0}\right)^{n_{_{\rm T}}}, \tag{3}$$

where the quantities $A_{_{\rm S}}$ and $A_{_{\rm T}}$ denote the amplitude of the scalar and tensor spectra, while $n_{_{\rm S}}$ and $n_{_{\rm T}}$ denote the corresponding spectral indices. The quantity k_0 is the pivot scale at which the amplitudes of the power spectra are quoted. Given the scalar and tensor spectra, the tensor-to-scalar ratio r is defined as the ratio of the latter to the former and, when comparing the power law case with the observations, it is the quantity r that is usually considered in lieu of the tensor amplitude $A_{_{\rm T}}$. Also, when considering the power law spectra, as is often done, we shall assume the slow roll consistency condition (viz. that $r = -8\,n_{_{\rm T}}$), so that the power law case is essentially described by the three parameters $A_{_{\rm S}}$, $n_{_{\rm S}}$ and r.

B. Evaluation of the background and the perturbations

We shall now outline the methods that we adopt to evolve the equations governing the background and the perturbations, and eventually evaluate the inflationary scalar and the tensor perturbation spectra.

Recall that, in a Friedmann universe, a canonical scalar field that is described by the potential $V(\phi)$ satisfies the following equation of motion:

$$\ddot{\phi} + 3\,H\,\dot{\phi} + V_{\phi} = 0, \tag{4}$$

where $V_{\phi} = (\mathrm{d}V/\mathrm{d}\phi)$, H is the Hubble parameter, while, as usual, the overdots denote differentiation with respect to the cosmic time coordinate. We solve the above differential equation exactly using the standard fourth order Runge-Kutta method, with e-folds as the independent variable. In the case of the chaotic inflationary model with sinusoidal modulations, we choose the initial value of the field to be $\phi_{_{\rm i}} \simeq 16$, while in the monodromy model, we set $\phi_{_{\rm i}} \simeq 12$. We then make use of the governing equations, considered under the slow roll approximation, to

determine the initial velocities of the field. These initial conditions allow sufficient number of e-foldings (say, about 60–70) before inflation ends near the bottom of the potentials. Further, following the convention, we shall choose the initial value of the scale factor to be such that the pivot scale $k_0 = 0.05\ \mathrm{Mpc}^{-1}$ leaves the Hubble radius at 50 e-folds before the end of inflation [12].

In the spatially flat Friedmann universe of our interest, the Fourier modes of the curvature perturbation R and the tensor perturbation h are described by the following equations [23, 24]:

$$R_k'' + 2\,\frac{z'}{z}\,R_k' + k^2\,R_k = 0 \quad \text{and} \quad h_k'' + 2\,\frac{a'}{a}\,h_k' + k^2\,h_k = 0, \tag{5}$$

where the overprimes denote differentiation with respect to the conformal time coordinate and $z = (a\,\dot{\phi}/H)$, with a being the scale factor. We impose the standard Bunch-Davies initial conditions on the perturbations when the modes are well inside the Hubble radius [say, when $(k/a\,H) = 100$], and evolve them using a Bulirsch-Stoer algorithm with an adaptive step size control routine [25]. We evaluate the scalar and the tensor perturbation spectra, viz.

$$\mathcal{P}_{_{\rm S}}(k) = \frac{k^2}{2\,\pi^2}\,|R_k|^2 \quad \text{and} \quad \mathcal{P}_{_{\rm T}}(k) = 8\,\frac{k^2}{2\,\pi^2}\,|h_k|^2, \tag{6}$$

at super Hubble scales, when the amplitude of the curvature and the tensor perturbations have frozen in [typically, when $(k/a\,H) \simeq 10^{-5}$].

C. Priors

As we mentioned, we shall assume the background cosmological model to be the standard, spatially flat, ΛCDM model. The model can be characterized by the following four parameters: $(\Omega_{\rm b}\,h^2)$, $(\Omega_{\rm c}\,h^2)$, θ and τ. The first two represent the baryon and the CDM densities (with h being related to the Hubble parameter), while the last two denote the ratio of the sound horizon to the angular diameter distance at decoupling and the optical depth to reionization, respectively. In Tab. I below, we have listed the priors that we work with on these four parameters.

Background parameter	Lower limit	Upper limit
$\Omega_{\rm b}\,h^2$	0.005	0.1
$\Omega_{\rm c}\,h^2$	0.01	0.99
θ	0.5	10.0
τ	0.01	0.8

TABLE I: The priors on the four parameters that describe the background, spatially flat, ΛCDM model. We keep the same priors on the background parameters for all the models and datasets that we consider.

As we had discussed earlier, we shall include the tensor perturbations in our analysis. When the slow roll consistency condition is imposed, the power law spectra are completely described by the scalar amplitude $A_{_{\rm S}}$, the scalar spectral index $n_{_{\rm S}}$ and the tensor-to-scalar ratio r. It is worth noting here that, in the inflationary models, the parameters that describe the potential determine the scalar *as well as* the tensor spectra entirely.

It is clear that, in the absence of oscillations in the potential, the two inflationary models of our interest will lead to nearly scale invariant spectra. Therefore, the main parameter that describes the two models, viz. m in the chaotic inflationary model and λ in the case of the axion monodromy model, are essentially determined by COBE normalization. In the absence of oscillations in the potential, we find that the best fit chaotic model leads to a power law spectrum with a scalar spectral index of about 0.96, while the monodromy model corresponds to $n_{_{\rm S}} \simeq 0.97$. Also, as one would have anticipated, both of them perform almost equally well against the data. However, when the oscillations in the potential are taken into account, they induce modulations in the slow roll parameters, which in turn lead to oscillations in the scalar power spectrum. (The tensor spectrum, though, is unaffected by these small oscillations, and remains nearly scale invariant.) As we shall see, when the oscillations are included, the monodromy model performs better against the data than the chaotic inflation model.

We have chosen the priors on the two inflationary models such that the amplitude of the resulting scalar spectra remain close to the COBE value, lead to the desired spectral index, and result in a certain minimum duration of inflation. We have listed the priors that we have worked with on the inflationary models in Tab. II.

Model	Parameter	Lower limit	Upper limit
Power law case	$\ln\,[10^{10}\,A_{_{\rm S}}]$	2.7	4.0
	$n_{_{\rm S}}$	0.5	1.5
	r	0.0	1.0
Chaotic model with sinusoidal modulation	$\ln\,[10^{10}\,m^2]$	-0.77	-0.58
	α	0	2×10^{-3}
	β	2×10^{-2}	1
	δ	$-\pi$	π
Axion monodromy model	$\ln\,[10^{10}\,\lambda]$	0.7	1.25
	α	1×10^{-5}	2×10^{-4}
	β	3×10^{-4}	1×10^{-3}
	δ	$-\pi$	π

TABLE II: The priors on the three parameters that describe the primordial spectra in the power law case, and the parameters that describe the two inflationary potentials of our interest. We work with the same priors when comparing the models with the WMAP as well as the ACT data.

D. Comparison with the recent CMB observations

To compare our models with the recent CMB observations, we perform the by-now common practice of the

Markov Chain Monte Carlo sampling of the parameter space using the publicly available CosmoMC package [26, 27]. The CosmoMC code in turn utilizes the CAMB code [28, 29] to arrive at the CMB angular power spectrum from given primordial scalar and tensor spectra. We evaluate the inflationary scalar as well as tensor spectra using an accurate and efficient numerical code (as outlined in Subsec. II B) and feed these primordial spectra into CAMB to obtain the corresponding CMB angular power spectra. We should stress here that we actually evolve *all the modes* that are required by CAMB from the sub to the super Hubble scales to obtain the perturbation spectra, rather than evolve for a smaller set of modes and interpolate to arrive at the complete spectrum. This becomes imperative in the models of our interest which (as one would expect, and as we shall illustrate below) contain fine features in the scalar power spectrum. It should be pointed out here that, while the chaotic model leads to a tensor-to-scalar ratio of 0.16, the monodromy model results in $r \simeq 0.06$. Though these tensor amplitudes are rather small to make any significant changes to the results, we have developed the code to evaluate the inflationary power spectra with future datasets (such as, say, Planck) in mind, and hence we nevertheless take the tensors into account exactly.

For our analysis, we consider the WMAP seven year data and the small scale data from ACT [3]. We have worked with the May 2010 versions of the CosmoMC and CAMB codes [26–29], and we have made use of the WMAP (version v4p1) and the ACT likelihoods while comparing with the corresponding data [30]. While ACT has observed CMB at the frequencies of 148 GHz as well as 218 GHz, we shall only consider the 148 GHz data. Moreover, though the ACT data spans over a wide range of multipoles ($500 \lesssim \ell \lesssim 10000$), for the sake of numerical efficiency (as has been implemented in Ref. [3]), we have set the CMB spectrum to zero for $\ell > 4000$, since the contribution at larger multipoles is negligible. When considering the ACT data, following the earlier work [3], in the power law case, we have marginalized over the three secondary parameters $A_{\rm SZ}$, $A_{\rm P}$ and $A_{\rm C}$, where $A_{\rm SZ}$ denotes the Sunyaev- Zeldovich amplitude, $A_{\rm P}$ the amplitude for the Poisson power from radio and infrared point sources, while $A_{\rm C}$ is the amplitude corresponding to the cluster power. However, when comparing the oscillatory inflationary potentials with the ACT data, we have only marginalized over $A_{\rm SZ}$ and have fixed the values of the other two parameters $A_{\rm P}$ and $A_{\rm C}$.

We should mention that we have taken gravitational lensing into account. Note that, to generate highly accurate lensed CMB spectra, CAMB requires $\ell_{\rm max\ scalar} \simeq (\ell_{\rm max} + 500)$, where $\ell_{\rm max}$ is, say, the largest multipole moment for which the data is available. The WMAP seven year data is available up to $\ell \simeq 1200$, while the ACT data is available up to $\ell \simeq 10000$. For the WMAP seven year data, we set $\ell_{\rm max\ scalar} \simeq 1800$, and for ACT we choose $\ell_{\rm max\ scalar} \simeq 4500$ since we are ignoring the data for $\ell > 4000$. We set $\ell_{\rm max\ tensor} \simeq 400$ for all the datasets, as they decay down quickly after that. ACT has measured only $C_\ell^{\rm TT}$, so the constraints from polarization, if any, will come only from the WMAP data.

III. RESULTS

In this section, we shall discuss the results of our analysis. We shall present the best fit values of the various parameters and also discuss the resulting primordial and CMB angular power spectra.

A. The best fit cosmological and inflationary parameters

We shall tabulate the best fit parameters in this subsection. We find that our results for the power law case are in good agreement with the WMAP seven year [2] and the ACT results [3]. In fact, we have cross checked our results with and without the tensor contribution. As stated earlier, we have made use of the three secondary parameters $A_{\rm SZ}$, $A_{\rm P}$ and $A_{\rm C}$ when comparing the power law case with the combined WMAP seven year and ACT data. In this case, we obtain the mean value of $A_{\rm P}$ to be 16.0, whereas $A_{\rm C}$ is described by a single tailed distribution which suggests that $A_{\rm C} < 8.4$ at 95% CL (when the tensors are not taken into account). We find that, for the power law spectra, if we fix $A_{\rm P}$ at the above-mentioned mean value and set $A_{\rm C}$ to be zero, the least squared parameter $\chi^2_{\rm eff}$ changes by a negligible amount (in fact, $\Delta\chi^2_{\rm eff} \simeq 0.2$-$0.3$), and the best fit, the mean values and the deviations too do not change appreciably. So, in the case of the two inflationary models of our interest, we have set $A_{\rm P} = 16.0$, $A_{\rm C} = 0$, and have marginalized over $A_{\rm SZ}$. In Tab. III below, we have listed the best fit values that we arrive at for the background cosmological parameters and the parameters that describe the chaotic inflationary model with superposed oscillations and the axion monodromy model.

B. The spectra and the improvement in the fit

In Tab. IV, we have listed the least squares parameter $\chi^2_{\rm eff}$ for the different models and datasets that we have considered. From the table it is clear that, the monodromy model leads to a much better fit to the data with $\chi^2_{\rm eff}$ improving by about 5-6. The table also seems to indicate two further points. Firstly, even though the chaotic model with the sinusoidal modulation does not perform as well as the monodromy model, the fact that the model performs better when the small scale data from ACT is included suggests that oscillations can be favored by the data. Secondly, oscillations of fixed amplitude in the potential as in the monodromy model seem to be more favored by the data than the oscillations of varying amplitude as in the case of the chaotic model with

	Datasets	WMAP-7	WMAP-7 + ACT
Model	Parameter	Best fit	Best fit
Chaotic model with sinusoidal modulation	$\Omega_{\rm b}\,h^2$	0.0222	0.0218
	$\Omega_{\rm c}\,h^2$	0.1155	0.1215
	θ	1.038	1.040
	τ	0.0917	0.0876
	$\ln\,\lfloor 10^{10}\,m^2\rfloor$	-0.7	-0.687
	α	1.21×10^{-3}	0.998×10^{-3}
	β	0.2914	0.2106
	δ	-2.1	-2.2
Axion monodromy model	$\Omega_{\rm b}\,h^2$	0.0229	0.0223
	$\Omega_{\rm c}\,h^2$	0.1144	0.1119
	θ	1.041	1.041
	τ	0.087	0.0884
	$\ln\,\lfloor 10^{10}\,\lambda\rfloor$	0.9489	0.9332
	α	1.66×10^{-4}	1.75×10^{-4}
	β	5.340×10^{-4}	5.42×10^{-4}
	δ	1.905	-0.6342

TABLE III: The best fit values for the two inflationary models on comparing with the WMAP seven year data (denoted as WMAP-7 here, and in the following table) alone, and along with the ACT data.

Datasets	WMAP-7	WMAP-7 + ACT
Model		
Power law case	7468.3	7500.4
Chaotic model with sinusoidal modulation	7467.6	7498.2
Axion monodromy model	7462.1	7495.2

TABLE IV: The $\chi^2_{\rm eff}$ for the different models and datasets that we have considered. Note that we have used the Gibbs approach in the WMAP likelihood code to calculate the $\chi^2_{\rm eff}$ for the CMB TT spectrum at the low multipoles (i.e. for $\ell < 32$) [1, 2].

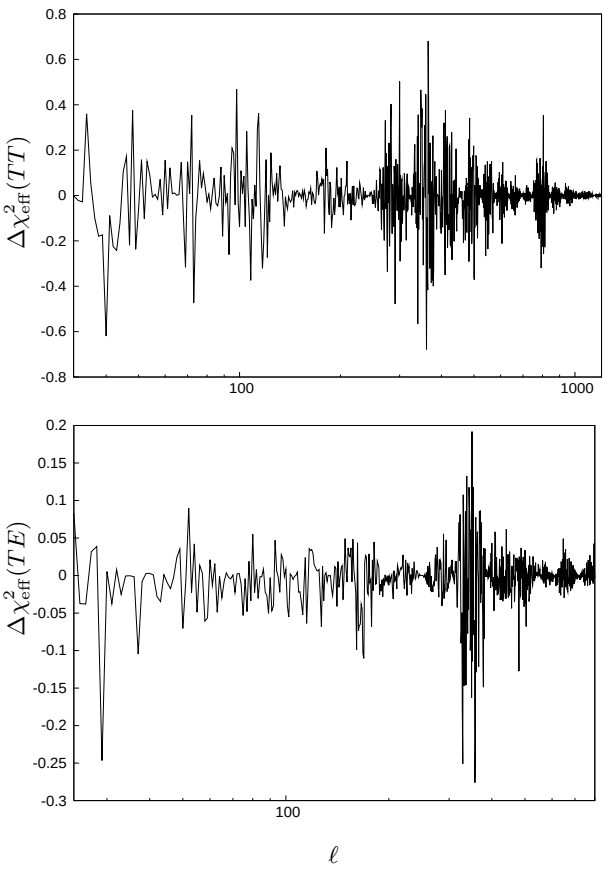

FIG. 1: The difference in $\chi^2_{\rm eff}$ with respect to the reference model, i.e. $\Delta\chi^2_{\rm eff} = [\chi^2_{\rm eff}({\rm model}) - \chi^2_{\rm eff}({\rm power\ law})]$, in the case of the axion monodromy model has been plotted as a function of the multipole moment for the WMAP seven year data. While the figure on top corresponds to the WMAP seven year TT data (for $\ell > 32$), the lower one is for the TE data (for $\ell > 24$).

sinusoidal modulations. In fact, this strengthens similar conclusions that has been arrived at earlier [18], wherein Planck scale oscillations of a certain amplitude in the primordial spectrum was found to lead to a considerably better fit to the data.

It is now interesting to enquire as to whether there exist localized windows of multipoles over which the improvement in the fit occurs. We find that, in the case of the chaotic model with sinusoidal modulations, as far as the WMAP seven year data is concerned, there is an improvement of at most unity in all the multipoles combined. For the monodromy model, the improvement at high and the low multipoles (i.e. $\ell < 32$) are almost equal (i.e. about 3) in the WMAP seven year TT data, and there is hardly any further improvement in the fit from the available TE and EE data. In Fig. 1, we have plotted the difference $\Delta\chi^2_{\rm eff} = [\chi^2_{\rm eff}({\rm model}) - \chi^2_{\rm eff}({\rm power\ law})]$ as a function of the multipoles for the WMAP seven year TT and TE data in the case of the axion monodromy model. It is clear from the figure that the source of the improvement in the fit is not confined to any specific set of multipoles, and it arises due to small increments that accrue over the entire range of available data. In Figs. 2 and 3, we have plotted the scalar power spectra and the corresponding CMB TT angular power spectra for the best fit values of the WMAP seven year data in the two inflationary models that we have considered. And, in Fig. 4, we have plotted the corresponding CMB EE angular power spectra and TE amplitude for all the models, including the power law case.

IV. CAN PLANCK SEE THE OSCILLATIONS?

In this section, we shall discuss the extent to which the data from Planck—that is expected to be coming forth in the very near future—will be able to constrain the presence and characteristics of extended features in the primordial spectrum.

Many of the parameters of inflationary models of the type that we are considering here can have a credible

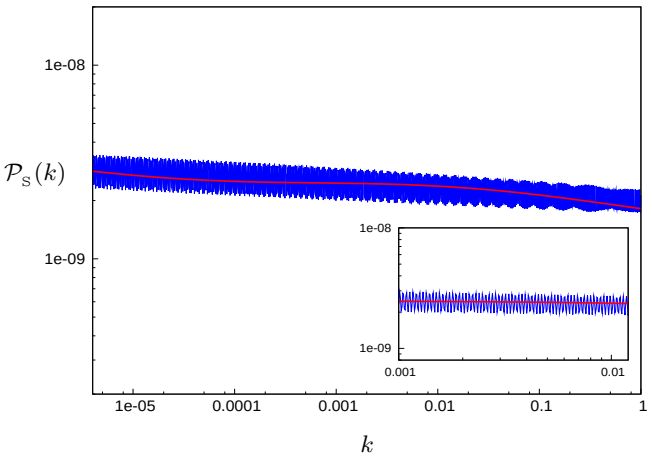

FIG. 2: The scalar power spectra corresponding to the best fit values of the WMAP seven year data for the two inflationary models that we have considered. The solid red and the solid blue lines describe the scalar power spectra in the cases of the chaotic model with a sinusoidal modulation and the axion monodromy model, respectively. The spectrum corresponding to the best fit power law model would essentially be same as in the chaotic model with sinusoidal modulations, but without any oscillations. Note the extraordinary extent of persistent oscillations in the case of the monodromy model.

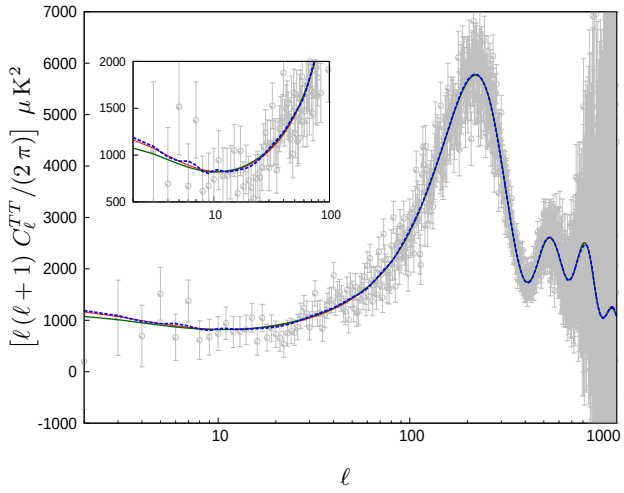

FIG. 3: The CMB TT angular power spectra corresponding to the best fit values of the different models for the WMAP seven year data. The solid red, solid green and the dashed blue curves correspond to the power law model, the chaotic model with sinusoidal modulation and the axion monodromy model, respectively. The gray circles with error bars denote the WMAP seven year *unbinned* data. The inset highlights the region where the discrimination between the various models is maximum. The difference in the angular power spectra between the various models is hardly visually evident. But, as we have discussed in the text, in the case of the axion monodromy model, the tiny and continued oscillations in the power spectrum lead to small improvements in the fit to the data over a wide range of multipoles, which eventually add up to a reasonable extent.

physical influence on the cosmological data, even if their presence has not yet been detected. It is expected that data from current missions such as Planck and beyond would be able to determine many of the presently unknown effects of the cosmological parameters. When performing a parameter error forecast for future observations, it is the Fisher matrix formalism that is commonly adopted. The error bars on the additional parameters are estimated from the derivatives of the observables with respect to the model parameters around the best fit point (for a discussion, see, for example, Ref. [31]). Such an analysis assumes that the likelihood of the cosmological parameters approximates a Gaussian multivariate. However, parameter degeneracies can occur where certain combinations of the parameters are not well constrained by the data. Also, the probability distribution of the parameters defined over a finite range may occasionally fail to converge at the boundaries. These lead to considerable deviations from the assumption of a multivariate Gaussian function.

We arrive at the possible constraints on the parameters using a different technique wherein we make suitable modifications to the CosmoMC code with a publicly available add-on code FuturCMB [32–34]. We firstly generate a simulated dataset for Planck, using a realistic noise model and the sky coverage fraction $f_{\rm sky}$. The CMB angular power spectrum generated from the best fit parameters of the models using the WMAP seven year data is treated as the fiducial power spectrum for generating the PLANCK mock data. We use this simulated data and incorporate the 'all_l_exact' data format in the CosmoMC code [35] to extract the projected parameter errors by sampling the likelihood and estimating the marginalized probability distribution in the parameter space. As we mentioned above, it is expected that this procedure would be more reliable than the Fisher matrix analysis since there is no assumption on the likelihood functions of these parameters being multivariate Gaussian distributions.

In Fig. 5, we have plotted the unbinned, CMB TT angular power spectrum of the Planck simulated data. To generate this mock data, we have considered the CMB TT angular power corresponding to the best fit parameters to the WMAP seven year data of the axion monodromy model (cf. Tab. III) as the fiducial power spectrum. We have plotted the resulting one dimensional distributions for the inflationary parameters in Fig. 6. The figure contains the constraints from the WMAP-7, WMAP-7 + ACT as well as the Planck simulated data for the original parameter m of the chaotic model and the frequency parameter β of the superimposed sinusoidal modulations. For the axion monodromy model, we have plotted the distributions for the initial parameter λ and the frequency parameter β for the same datasets. Fig. 7 contains the two dimensional contour plots for the above-

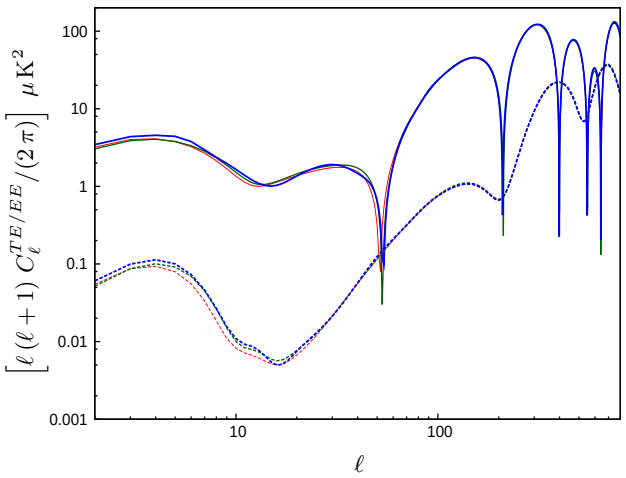

FIG. 4: The CMB TE and the EE angular power spectra corresponding to the best fit values of the different models for the WMAP seven year data. The solid red, green and blue curves represent the TE spectrum (in fact, its magnitude) in the power law case, the chaotic model with sinusoidal modulations and the axion monodromy model, respectively. The dashed curves denote the corresponding EE angular power spectra.

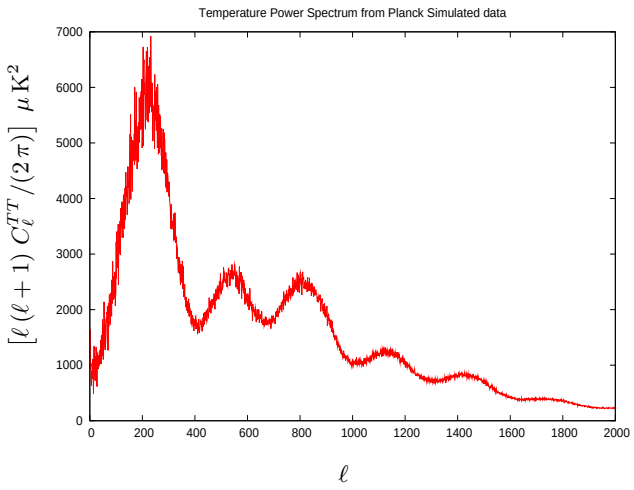

FIG. 5: The CMB TT angular power spectrum of the unbinned Planck simulated data which has been generated from the fiducial, best fit CMB spectrum (to WMAP-7) of the axion monodromy model.

mentioned set of parameters. Again, we have displayed the constraints from all the three datasets. It can be easily perceived from these set of figures that the Planck data leads to much tighter bounds on the inflationary parameters than the currently available data for the same range of priors for the various parameters.

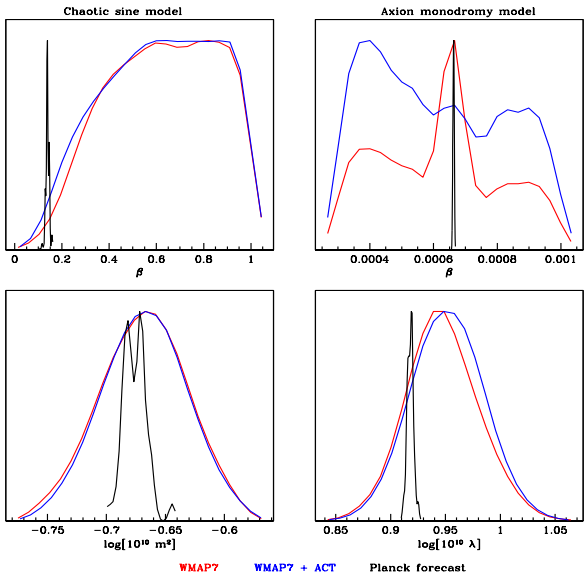

FIG. 6: One dimensional distributions of the inflationary model parameters from the WMAP-7, WMAP-7 + ACT and the Planck simulated data. We have plotted the constraints on the parameters m and β of the chaotic model with sinusoidal modulations (on the left column) and the parameters λ and β for the axion monodromy model (on the right column). It is evident that the simulated Planck data tightens the bounds on the parameters substantially.

V. DISCUSSION

In this work, our main aim has been to investigate if the CMB data support certain non-local features—i.e. a certain repeated and characteristic pattern that extends over a wide range of scales—in the primordial scalar power spectrum. With this goal in mind, we have studied two models of inflation, both of which contain oscillatory terms in the inflaton potential. The oscillations in the potential produces oscillations in the slow roll parameters, which in turn generate oscillations in the primordial as well as the CMB power spectra. Earlier work in this context had utilized the analytical expressions for the primordial power spectra, obtained in the slow roll approximation, to compare such models with the data [19–21]. Instead, we have used an accurate and efficient numerical code to arrive at the inflationary scalar and tensor power spectra. In fact, in order to ensure that a good level of accuracy, rather than evolve a finite set of modes and interpolate, we have evolved and computed the inflationary perturbation spectra for all the modes that is required by CAMB to arrive at the corresponding CMB angular power spectra. While this reflects the extent of the numerical accuracy of our computations, the efficiency of the code can be gauged by the fact that we have able to been able to complete the required runs within a reasonable amount of time despite such addi-

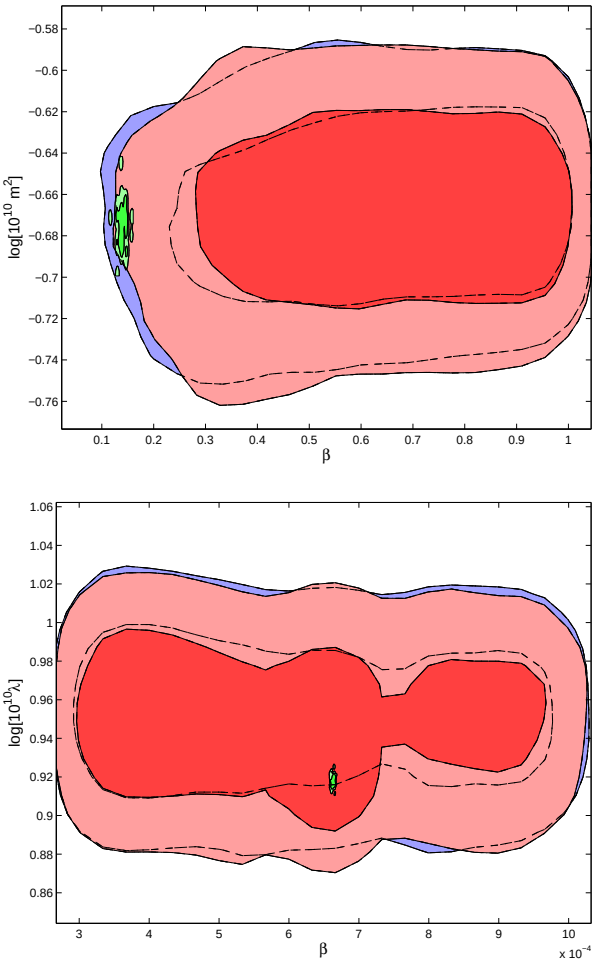

FIG. 7: The joint two dimensional constraints on the inflationary model parameters from the WMAP-7, WMAP-7 + ACT and the Planck simulated data. The figure on top illustrates the joint constrains on the parameters m and β that characterize the chaotic model with sinusoidal modulations, while the lower figure displays the joint constraints on the parameters λ and β that describe the axion monodromy model. Note that the red contours are the 1-σ and the 2-σ constraints from WMAP-7, the blue contours are from WMAP-7 + ACT, while the green contours are from the simulated Planck data. (The broken black lines on the red contours are traces of the underlying blue contours from the WMAP-7 + ACT data.) It is again clear that the simulated Planck data constrains the parameters considerably more than the available data.

tional demands.

Prior experience, gained in a different context, had already suggested the possibility that small and continued oscillations in the scalar power spectra can lead to a better fit to the data [18]. This experience has been corroborated by the earlier [19–21] and our current analysis. We find that, oscillations, such as those occur in the axion monodromy model lead to a superior fit to the data. We should, however, mention here that our numerical analysis indicates that the extent of the improvement does not amount to as much as it has been pointed to in the analytical approaches. While the analytical efforts had pointed to an improvement of about 11 or so in the least squared parameter $\chi^2_{\rm eff}$ for the axion monodromy model, we find an improvement of about 6.

In addition to comparing with the already available data, we have also discussed on the extent to which Planck may be able to constrain the parameters that describe the oscillatory terms in the potential. Rather than adopt the standard method of forecasting for the model parameters using the Fisher matrix, we have been able to arrive at the constraints with suitable modifications to CosmoMC. We believe that the method we have adopted is more reliable than the Fisher matrix approach which does not work equally well when the parameters are not described by multivariate Gaussian distributions. The one-dimensional marginalized distributions and the two-dimensional contours for the parameters of the inflationary models that we have arrived at show that future full sky CMB data sets such as Planck would be capable of narrowing the constraints on these parameters considerably.

Acknowledgments

We acknowledge the use of the high performance computing facilities at the Harish-Chandra Research Institute, Allahabad, India, as well as at the Inter-University Centre for Astronomy and Astrophysics, Pune, India. TS and MA acknowledge support from the Swarnajayanti Fellowship, Department of Science and Technology, India. DKH would like to thank Sanjoy Biswas for useful discussions on numerical procedures. We would also like to acknowledge the use of the CosmoMC package [26], and the data products provided by the WMAP science team [30], the ACT and the Planck missions.

[1] J. Dunkley *et al.*, Astrophys. J. Suppl. **180**, 306 (2009); E. Komatsu *et al.*, Astrophys. J. Suppl. **180**, 330 (2009).
[2] D. Larson *et al.*, Astrophys. J. Suppl. **192**, 16 (2011); E. Komatsu *et al.*, Astrophys. J. Suppl. **192**, 18 (2011).
[3] J. Dunkley *et al.*, arXiv:1009.0866v1 [astro-ph.CO].
[4] J. Martin, C. Ringeval and R. Trotta, arXiv:1009.4157v3 [astro-ph.CO].
[5] See, `http://www.sciops.esa.int/PLANCK/`.
[6] See, `http://www.core-mission.org/`.
[7] S. Hannestad, Phys. Rev. D **63**, 043009 (2001); S. L. Bridle, A. M. Lewis, J. Weller and G. Efstathiou, Mon. Not. Roy. Astron. Soc. **342**, L72 (2003); P. Mukherjee and Y. Wang, Astrophys. J. **599**, 1 (2003); S. Hannestad, JCAP **0404**, 002 (2004); A. Shafieloo and T. Souradeep,

Phys. Rev. D **70**, 043523 (2004); D. Tocchini-Valentini, Y. Hoffman and J. Silk, Mon. Not. Roy. Astron. Soc. **367**, 1095 (2006); A. Shafieloo, T. Souradeep, P. Manimaran, P. K. Panigrahi and R. Rangarajan, Phys. Rev. D **75**, 123502 (2007); A. Shafieloo and T. Souradeep, Phys. Rev. D **78**, 023511 (2008); R. Nagata and J. Yokoyama, Phys. Rev. D **79**, 043010 (2009); G. Nicholson and C. R. Contaldi, JCAP **0907**, 011 (2009).

[8] M. Bridges, F. Feroz, M. P. Hobson and A. N. Lasenby, Mon. Not. Roy. Astron. Soc. **400**, 1075 (2009); H. V. Peiris and L. Verde, Phys. Rev. D **81**, 021302 (2010); Z.-K. Guo, D. J. Schwarz and Y. -Z. Zhang, arXiv:1105.5916v1 [astro-ph.CO].

[9] H. V. Peiris *et al.*, Astrophys. J. Suppl. **148**, 213 (2003).

[10] B. Feng and X. Zhang, Phys. Lett. B **570**, 145 (2003); M. Kawasaki and F. Takahashi, Phys. Lett. B **570**, 151 (2003); R. Sinha and T. Souradeep, Phys. Rev. D **74**, 043518 (2006); M. J. Mortonson and W. Hu, Phys. Rev. D **80**, 027301 (2009).

[11] R. K. Jain, P. Chingangbam, J.-O. Gong, L. Sriramkumar and T. Souradeep, JCAP **0901**, 009 (2009); R. K. Jain, P. Chingangbam, L. Sriramkumar and T. Souradeep, Phys. Rev. D **82**, 023509 (2010).

[12] L. Covi, J. Hamann, A. Melchiorri, A. Slosar and I. Sorbera, Phys. Rev. D **74**, 083509 (2006); J. Hamann, L. Covi, A. Melchiorri and A. Slosar, Phys. Rev. D **76**, 023503 (2007); M. Joy, V. Sahni and A. A. Starobinsky, Phys. Rev. D **77**, 023514 (2008); M. Joy, A. Shafieloo, V. Sahni and A. A. Starobinsky, JCAP **0906**, 028 (2009); M. J. Mortonson, C. Dvorkin, H. V. Peiris and W. Hu, Phys. Rev. D **79**, 103519 (2009); D. K. Hazra, M. Aich, R. K. Jain, L. Sriramkumar and T. Souradeep, JCAP **1010**, 008 (2010).

[13] P. Hunt and S. Sarkar, Phys. Rev. D **70**, 103518 (2004); Phys. Rev. D **76**, 123504 (2007); M. Kawasaki, F. Takahashi and T. Takahashi, Phys. Letts. B **605**, 223 (2005); J.-O. Gong, JCAP **0507**, 015 (2005); M. Kawasaki and K. Miyamoto, arXiv:1010.3095v2 [astro-ph.CO]; A. Achucarro, J.-O. Gong, S. Hardeman, G. A. Palma and S. P. Patil, JCAP **1101**, 030 (2011); K. Kumazaki, S. Yokoyama and N. Sugiyama, arXiv:1105.2398v1 [astro-ph.CO].

[14] A. A. Starobinsky, Sov. Phys. JETP Lett. **55**, 489 (1992).

[15] C. Dvorkin and W. Hu, Phys. Rev. D **81**, 023518 (2010).

[16] W. Hu, arXiv:1104.4500v1 [astro-ph.CO].

[17] J. M. Cline, P. Crotty and J. Lesgourgues, JCAP **0309**, 010 (2003); C. R. Contaldi, M. Peloso, L. Kofman and A. Linde, JCAP **0307**, 002 (2003); L. Sriramkumar and T. Padmanabhan, Phys. Rev. D **71**, 103512 (2005); D. Boyanovsky, H. J. de Vega and N. G. Sanchez, Phys. Rev. D **74**, 123006 (2006); Phys. Rev. D **74**, 123007 (2006); B. A. Powell and W. H. Kinney, Phys. Rev. D **76**, 063512 (2007); C. Destri, H. J. de Vega and N. G. Sanchez, Phys. Rev. D **78**, 023013 (2008).

[18] J. Martin and C. Ringeval, Phys. Rev. D **69**, 083515 (2004); Phys. Rev. D **69**, 127303 (2004); JCAP **0501**, 007 (2005); M. Zarei, Phys. Rev. D **78**, 123502 (2008).

[19] C. Pahud, M. Kamionkowski and A. R. Liddle, Phys. Rev. D **79**, 083503 (2009).

[20] R. Flauger, L. McAllister, E. Pajer, A. Westphal and G. Xu, JCAP **1006**, 009 (2010); R. Flauger and E. Pajer, JCAP **1101**, 017 (2011).

[21] T. Kobayashi and F. Takahashi, JCAP **1101**, 026 (2011).

[22] S. Hannestad, T. Haugboelle, P. R. Jarnhus and M. S. Sloth, JCAP **1006**, 001 (2010).

[23] B. Bassett, S. Tsujikawa and D. Wands, Rev. Mod. Phys. **78**, 537 (2006).

[24] L. Sriramkumar, Curr. Sci. **97**, 868 (2009).

[25] W. H. Press, S. A. Teukolsky, W. T. Vetterling and B. P. Flannery, *Numerical Recipes in FORTRAN 90*, Second edition (Cambridge University Press, Cambridge, England, 1996).

[26] See, `http://cosmologist.info/cosmomc/`.

[27] A. Lewis and S. Bridle, Phys. Rev. D **66**, 103511 (2002).

[28] See, `http://camb.info/`.

[29] A. Lewis, A. Challinor and A. Lasenby, Astrophys. J. **538**, 473 (2000).

[30] See, `http://lambda.gsfc.nasa.gov/`.

[31] S. Dodelson, *Modern Cosmology* (Academic Press, San Diego, U.S.A., 2003).

[32] See, `http://lpsc.in2p3.fr/perotto/`.

[33] L. Perotto, J. Lesgourgues, S. Hannestad, H. Tu and Y. Y. Wong, JCAP **0610**, 013 (2006).

[34] C. Pahud, A. R. Liddle, P. Mukherjee and D. Parkinson, Phys. Rev. D **73**, 123524 (2006).

[35] See the discussion page on the CosmoCoffee web-site, `http://cosmocoffee.info/viewtopic.php?t=231`.